Optical Spin Hall Effect

Alexey Kavokin,[1,2] Guillaume Malpuech,[2] and Mikhail Glazov[2,3]

[1]*Department of Physics and Astronomy, University of Southampton, SO17 1BJ Southampton, United Kingdom*
[2]*LASMEA, Université Blaise Pascal, 24 Avenue des Landais, 63177 Aubiere, France*
[3]*A. F. Ioffe Physico-Technical Institute, 26 Politechnicheskaya, 194021 St. Petersburg, Russia*

(Received 10 May 2005; published 19 September 2005)

A remarkable analogy is established between the well-known spin Hall effect and the polarization dependence of Rayleigh scattering of light in microcavities. This dependence results from the strong spin effect in elastic scattering of exciton polaritons: if the initial polariton state has a zero spin and is characterized by some linear polarization, the scattered polaritons become strongly spin polarized. The polarization in the scattered state can be positive or negative dependent on the orientation of the linear polarization of the initial state and on the direction of scattering. Very surprisingly, spin polarizations of the polaritons scattered clockwise and anticlockwise have different signs. The optical spin Hall effect is possible due to strong longitudinal-transverse splitting and finite lifetime of exciton polaritons in microcavities.

DOI: 10.1103/PhysRevLett.95.136601 PACS numbers: 72.25.Fe, 71.36.+c, 72.25.Rb, 78.35.+c

The spin Hall effect (SHE) had been proposed by Dyakonov and Perel' in 1971 [1]. It was revisited and has attracted a lot of attention in the last five years after its rediscovery by Hirsch in 1999 [2] and the suggestion of the so-called *intrinsic* SHE by two groups in 2003 and 2004 [3,4]. The SHE is now largely studied theoretically and experimentally [5]. The spin Hall effect is the spin current induced by the electric current. One can distinguish between the extrinsic and intrinsic SHE, first one due to elastic spin-flip scattering of carriers with impurities and second one due to the spin-splitting of conduction band induced by the spin-orbit interaction. The SHE has a huge potentiality for spintronics and quantum informatics, as many works show [6].

In this work, we demonstrate theoretically that the extrinsic SHE has a remarkable analogy in semiconductor optics, namely, in Rayleigh scattering of light in microcavities. The spin polarization in the scattered state can be positive or negative dependent on the orientation of the linear polarization of the initial state and on the angle of rotation of the polariton wave vector during the act of scattering. Very surprisingly, spin polarizations of the polaritons scattered clockwise and anticlockwise have different signs. Despite the visible similarity with the electronic extrinsic SHE, the optical SHE has a different physical mechanism which reminds to some extent that of the intrinsic SHE. The optical SHE is possible due to strong longitudinal-transverse splitting and finite lifetime of exciton polaritons (polaritons) in microcavities. The effect we propose should not be confused with the ''Hall effect of light'' or ''optical Hall effect'' proposed in Refs. [7,8], which consist in the drift of a wave packet of light in a media having a gradient of the refractive index [7], or in the presence of the magnetic field [8].

We consider a semiconductor microcavity in the strong-coupling regime between the optical mode of the cavity and the heavy hole excitons of the embedded quantum wells (QWs) [9]. In this regime, new eigenmodes appear called polaritons. They are characterized by two branches of in-plane dispersion which are splitted by so-called vacuum-field Rabi splitting. We shall refer to the familiar experimental configuration of the resonant Rayleigh scattering [10]. We shall suppose that one of the $\vec{k} \neq 0$ states of the lower polariton branch (LPB) is resonantly excited by a linearly polarized light [$\vec{k} = (k_x, k_y)$ is the in-plane polariton wave vector] [see the scheme in Fig. 1(a)]. The elastically scattered signal comes from the quantum states whose wave vector is rotated with respect to the initial $\vec{k}$ by some nonzero angle θ. We shall study polarization of the scattered light as a function of θ and k.

We shall use the *pseudospin* model [11] that describes the dynamics of polarization of polaritons in microcavities. The pseudospin is a three-dimensional vector. Its in-plane components describe both linear polarization orientations in a given polariton state, while its normal-to-plane component s_z is proportional to the circular polarization of the polariton state and hence the total average spin of polaritons in the given quantum state.

It has been shown theoretically [11] and experimentally [12,13] that the main mechanism of spin relaxation of polaritons in microcavities in the linear regime (i.e., if polariton-polariton interactions are not important) is the pseudospin precession induced by the longitudinal-transverse splitting of polaritons. This splitting (Δ_{LT}) gives rise to an effective magnetic field H_{eff} oriented in plane of the microcavity which rotates the polariton pseudospin if the latter is not parallel to it [11]. Taking into account this effect, propagation of the polaritons in microcavities can be described by the following effective Hamiltonian:

$$\hat{H} = \frac{\hbar^2 k^2}{2m^*} + \mu_B g(\boldsymbol{\sigma} \mathbf{H}_{\mathrm{eff}}), \qquad (1)$$

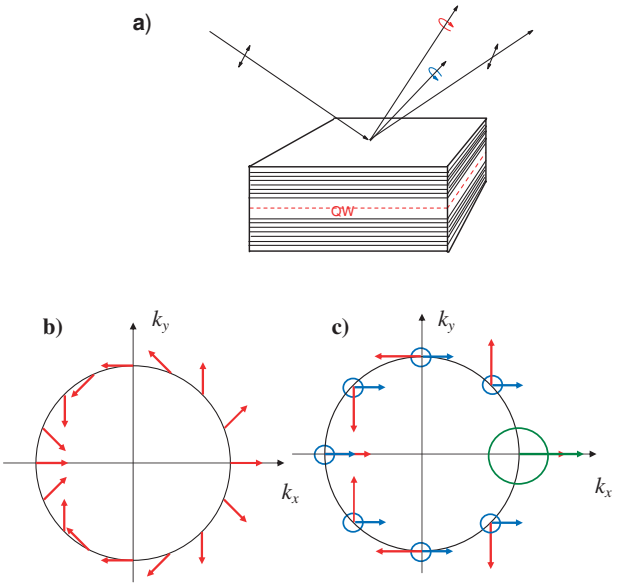

FIG. 1 (color). (a) Scheme of the considered experimental configuration: linearly polarized light is incident on a semiconductor microcavity under oblique angle. Polarization of the scattered light is analyzed. (b) The red arrows show the distribution of the effective magnetic field induced by the TE-TM splitting on an elastic circle in reciprocal space. (c) The green circle sketches the polariton state resonantly excited by a pulse having an in-plane wave vector along the x axis. This initial polariton state is TM polarized and has its pseudospin parallel to the x direction (green arrow). The blue circles and blue arrows show the short-time distribution of particles and their pseudospin orientation. The red arrows show the distribution of the effective magnetic field induced by the TE-TM splitting.

where m^* is the polariton effective mass, $\boldsymbol{\sigma}$ is the Pauli matrix vector, the effective magnetic field $\mathbf{H}_{\text{eff}} = \frac{\hbar}{\mu_B g}\boldsymbol{\Omega}_{\mathbf{k}}$, and $\boldsymbol{\Omega}_{\mathbf{k}}$ has the following components:

$$\Omega_x = \frac{\Omega}{k^2}(k_x^2 - k_y^2), \qquad \Omega_y = 2\frac{\Omega}{k^2}k_x k_y, \tag{2}$$

with $\Omega = \frac{\Delta_{\text{LT}}}{\hbar}$. The orientation of the effective field with respect to the in-plane polariton wave vector is shown in Fig. 1(b).

Let us assume that light is incident in the (x, z) plane. In the reciprocal space, it excites resonantly a polariton state having an in-plane wave vector directed along the x axis, as shown in green in Fig. 1(c). This polariton state is polarized in the xz plane (TM polarization), which means that its pseudospin $\mathbf{s_0}$ is parallel to the x axis. As the pseudospin is parallel to the effective field, it does not experience any precession at the initial point. Consider now the scattering act which brings our polariton into the state (k_x', k_y'), with $k_x' = k\cos\theta$ and $k_y' = k\sin\theta$. Following the classical theory of Rayleigh scattering [14], we assume that the polarization does not change during the scattering act, so that at the beginning the pseudospin of the scattered state keeps oriented in the x direction [Fig. 1(c)]. As the effective field is no more parallel to the pseudospin, it starts precessing. One can note that the precession takes place in opposite directions for two opposite scattering angles. Figure 2 shows schematically the resulting dependence of the circular polarization degree of light scattered by the cavity in different directions. Red (blue) corresponds to the right (left) circularly polarized light. One can note the inequivalence of clockwise and anticlockwise scattering: if the spin-up majority of polaritons (right-circular polarization) dominates scattering at the angle θ, the signal at angle $-\theta$ is mostly emitted by spin-down polaritons (left-circular polarization), and vice versa. In order to obtain the polarization distribution in scattering of TE-polarized light (incident electric field in the y direction), one should simply interchange the blue and red in Fig. 2. This effect can be detected experimentally by measuring the circular polarization degree of the scattered light versus the scattering angle. Note that in the four directions corresponding to the boarders between the blue and red areas the linear polarization of light is conserved. An experimental observation of conservation of the linear polarization in the four directions and its modification in the areas between them have been recently reported by Langbein [15], which represents indirect evidence of the effect we propose.

This analysis can be made more quantitative by writing the equation of motion for the pseudospin of a scattered state which reads

$$\frac{\partial \mathbf{s}}{\partial t} = \mathbf{s} \times \boldsymbol{\Omega}_{\mathbf{k}'} + \mathbf{f}(t) - \frac{\mathbf{s}}{\tau}, \tag{3}$$

where the first term describes precession and the second term describes the flux of polaritons coming from the initial state. It has only the x component (or the y compo-

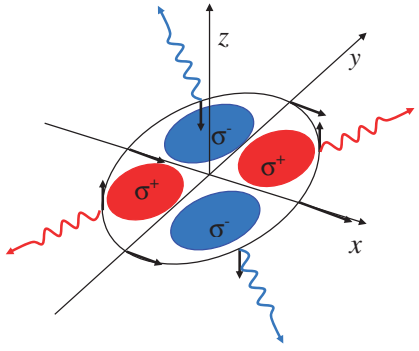

FIG. 2 (color). The black arrows show the polariton pseudospin orientation in the reciprocal space at a time $t = \frac{\pi}{2\Omega}$ after arrival of the TM-polarized excitation pulse. In the first and third quarter (emission angles $[0°-90°]$ and $[180°-270°]$, respectively) polaritons have their pseudospins parallel to the z direction, which corresponds to the right-circularly polarized emission (σ^+), shown in red. In the second and fourth quarter (emission angles $[90°-180°]$ and $[270°-360°]$, respectively) the polariton pseudospins are antiparallel to the z axis, which corresponds to the left-circularly polarized emission (σ^-), shown in blue.

nent), as the pseudospin in the initial state is always parallel to the x axis (y axis) for TM-polarized (TE-polarized) excitation, $\mathbf{f}(t) = \frac{\mathbf{s_0}}{\tau_1} e^{-t/\tau}$, with τ_1 being the elastic scattering time-constant. The last term in Eq. (3) accounts for the finite polariton lifetime τ. The polariton population dynamics at the scattered state is described by a simple rate equation:

$$\frac{\partial N}{\partial t} = 2\frac{s_0}{\tau_1} e^{-t/\tau} - \frac{N}{\tau}. \tag{4}$$

Solutions of Eqs. (3) and (4) with the initial condition $N = 0$ for the z component of the pseudospin yield

$$\begin{aligned} s_z(t,\theta) &= \pm s_0 \frac{\Omega_y(\theta)}{\Omega^2 \tau_1} e^{-t/\tau}[1 - \cos\Omega t], \\ N &= 2\frac{s_0 t}{\tau_1} e^{-t/\tau}. \end{aligned} \tag{5}$$

Here and further "+" holds for TM excitation and "−" holds for TE excitation.

The circular polarization degree of light emitted by the cavity from the given polariton state is

$$\rho_c = \frac{2s_z}{N}. \tag{6}$$

For our scattered state, it writes

$$\rho_c(t,\theta) = \pm \frac{\Omega_y(\theta)[1 - \cos\Omega t]}{2\Omega^2 t}. \tag{7}$$

The time-averaged value for the circular polarization is

$$\rho_c(\theta) = 2\frac{\int_0^\infty s_z(t,\theta)dt}{\int_0^\infty N(t)dt} = \pm \frac{\Omega\tau \sin 2\theta}{1 + \Omega^2\tau^2}. \tag{8}$$

Equation (8) shows that the maximum value of $|\rho_c|$ is $1/2$, and it is achieved when $\Omega\tau = 1$ and for $\theta = 45°, -135°$ for TM excitation and for and $\theta = -45°, 135°$ for TE excitation. The minimum value $\rho_c = -1/2$ is achieved at the angles symmetric to the above ones (see Fig. 2).

For numerical modeling, we consider a realistic GaAs based microcavity containing six 20 nm wide GaAs QWs. The distributed Bragg reflectors are made of $AlAs/Al_{0.1}Ga_{0.9}As$ with 17 and 27 pairs in the upper and lower mirror, respectively. The vacuum-field Rabi splitting in such structures is about 8 meV. The LPB calculated for the exciton-cavity mode detuning of -11 meV is shown in Fig. 3(a). The wave-vector dependence of Δ_{LT} calculated using the transfer matrix technique is shown in Fig. 3(b). It shows a maximum of about 0.1 meV at $k = 2.5 \times 10^6$ m^{-1}. For such a structure the width of the bare cavity mode is 0.16 meV, which corresponds to the cavity photon lifetime $\tau_{ph} = 4.1$ ps. The polariton lifetime is essentially radiative in the photonic part of the polariton dispersion and is given by $\tau \approx \frac{\tau_{ph}}{C}$, where C is the photon fraction of the polariton mode. The Rayleigh scattering time constant τ_1 for the polariton mode is linked with the inhomogeneous broadening Δ of the bare exciton line by $\tau_1 \approx \frac{1-C}{\Delta}\hbar$.

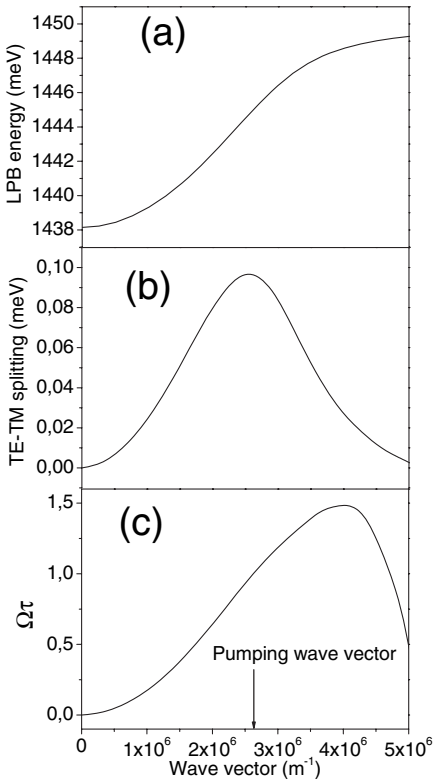

FIG. 3. (a) Dispersion of the LPB in the model microcavity. The bare exciton energy is 1450 meV, and the bare photon energy at $k = 0$ is 1439 meV. (b) Wave-vector dependence of the energy splitting Ω between TE- and TM-polarized polariton modes. (c) Wave-vector dependence of the product $\Omega\tau$, where τ is the polariton radiative lifetime.

The typical values of Δ in these kind of structures are of the order of 50 μeV [10], which yields $\tau_1 \approx 40$ ps. This is much longer than the polariton lifetime, which allows us to safely neglect multiple-scattering processes. Figure 3(c) shows the wave-vector dependence of the product $\Omega\tau$. It reaches one at $k_0 = 2.6 \times 10^6$ m^{-1}, which corresponds to the incidence angle of 20°. The state corresponding to this incidence angle also has the advantage to be apart both from the bare exciton resonance and from the "magic angle" [16]. Therefore, the corresponding polariton states are only very weakly affected by phonon scattering and polariton-polariton scattering. In the low density limit for these states, elastic scattering by disorder (Rayleigh scattering) is the main scattering mechanism.

Figure 4(a) shows the time dependence of circular polarization degree $\rho_c(t)$ for the signal scattered at +45° and −45° calculated for the incident wave vector k_0 at the TM-polarized excitation. Both curves oscillate with a frequency Ω and decay with a characteristic time Ω^{-1}. The only difference between them is the sign. The inset shows the time evolution of the population of these states. Figure 4(b) shows the time-averaged circular polarization degree versus the scattering angle for two values of the incident light wave vector (k_0 and $k_0/2$). The curves are antisymmetric

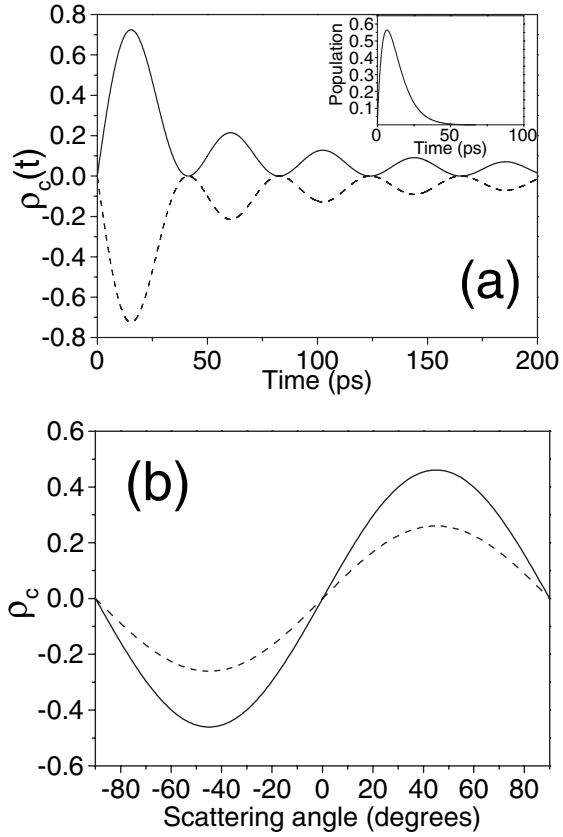

FIG. 4. (a) Time dependence of the circular polarization degree of light emitted by the states whose in-plane wave vector makes an angle θ of $+45°$ (solid line) and $-45°$ (dashed line) with respect to the wave vector of the incident light. The inset shows the time dependence of the populations of the corresponding states. (b) Integrated circular polarization degree versus the scattering angle θ for two different in-plane wave vectors of the incident light, namely, 2.6×10^6 m^{-1} (solid line) and 1.3×10^6 m^{-1} (dashed line).

with respect to the zero-angle direction. Within the $-90°$ to $+90°$ range of angles, the circular polarization achieves its maximum absolute value for the scattering angles of $+45°$ and $-45°$. This maximum varies between 0.25 and 0.5, depending on the incident wave vector.

Let us discuss at this point the similarity of the optical spin Hall effect with intrinsic and extrinsic electronic SHEs. Our effective Hamiltonian (1) is formally equivalent to the electronic Hamiltonian containing the spin-orbit interaction (Rashba or Dresselhaus) term leading to the intrinsic SHE [4], while the wave-vector dependence of our effective magnetic field and the Rashba field is different. The similarity of Hamiltonians allows us to suggest that the optical spin Hall effect we describe is similar to the intrinsic rather than extrinsic electronic SHE. In the intrinsic SHE for electrons, an external field is needed to change the particle's wave vector and thus to create a spin polarized flux. In our case, the Rayleigh scattering of light plays the role of the field changing the polariton wave vector. On the other hand, the Rayleigh scattering in the optical SHE seems analogous to the impurity scattering of electrons in the extrinsic SHE, which allows us to suggest that our effect has also common features with the extrinsic effect. An essential difference between optical SHE and extrinsic electronic SHE comes from the fact that the Rayleigh scattering of light is isotropic and *polarization independent*, while the impurity scattering of electrons is anisotropic and *spin sensitive* [1,2]. In our case, spin polarization of scattered polaritons is gained after the scattering act, while in the extrinsic SHE the electron spin flips during the scattering act.

Finally, the optical spin Hall effect we described invokes the scattering of particles by a static disorder. However, a similar effect can be expected for the acoustic phonon assisted scattering which follows the same spin conservation rules as the Rayleigh scattering [9]. Therefore the similar angle dependence of the circular polarization of the scattered light might be observed at upper or lower energies.

In conclusion, the optical spin Hall effect consists of the polarized Rayleigh scattering of light having an antisymmetric angular dependence. At linearly polarized excitation, the scattered signal gets circularly polarized, which means that photons gain a nonzero average spin. The orientation of this spin is critically sensitive to the direction of scattering and the orientation of the linear polarization of the exciting light. We foresee various applications in optical switches as well as for creation of polarization entangled photon pairs.

This work has been supported by the Marie-Curie research-training network "Clermont2," Contract No. MRTN-CT-2003-503677, and RFBR.

[1] M. I. Dyakonov and V. I. Perel', Phys. Lett. **35A**, 459 (1971).
[2] J. E. Hirsch *et al.*, Phys. Rev. Lett. **83**, 1834 (1999).
[3] S. Murakami *et al.*, Science **301**, 1348 (2003).
[4] J. Sinova *et al.*, Phys. Rev. Lett. **92**, 126603 (2004).
[5] See, e.g., C. Day, Phys. Today **58**, No. 02, 17 (2005).
[6] Y. Kato *et al.*, Science **306**, 1910 (2004); J. Wunderlich *et al.*, Phys. Rev. Lett. **94**, 047204 (2005).
[7] M. Onoda *et al.*, Phys. Rev. Lett. **93**, 083901 (2004).
[8] J. Singh *et al.*, Phys. Rev. A **61**, 025402 (2000).
[9] A. Kavokin and G. Malpuech, *Cavity Polaritons* (Elsevier, Amsterdam, 2003).
[10] W. Langbein *et al.*, Phys. Rev. Lett. **88**, 47401 (2002).
[11] K. Kavokin *et al.*, Phys. Rev. Lett. **92**, 017401 (2004).
[12] M. D. Martin, Phys. Rev. Lett. **89**, 77 402 (2002).
[13] I. Shelykh *et al.*, Phys. Rev. B **70**, 035320 (2004).
[14] Lord Rayleigh (J. W. Strutt), Philos. Mag. **47**, 375 (1899).
[15] W. Langbein, in *Proceedings of the 26th International Conference on Physics of Semiconductors* (Institute of Physics, Bristol, 2003), p. 112.
[16] P. G. Savvidis *et al.*, Phys. Rev. Lett. **84**, 1547 (2000).